



# Green and Chemically Prepared Zinc Sulfide Nanoparticles: A Comparative Study

A.H. Al-Hammadi<sup>1</sup>, Annas Al-Sharabi<sup>2</sup>, Adnan Alnehia<sup>1,2\*</sup>

1. Department of Physics, Faculty of Sciences, Sana'a University, Sana'a, 12081, Yemen.

2. Department of Physics, Faculty of Applied Sciences, Thamar University, Dhamar 87246, Yemen.

\*Correspondence: [ad.alnehia@su.edu.ye](mailto:ad.alnehia@su.edu.ye)

## ARTICLE INFO

Article history:

Received: December 23, 2022

Accepted: January 28, 2023

Published: January, 2023

## Keywords

1. green synthesis
2. *Plectranthus barbatus*,
3. optical
4. ZnS

**ABSTRACT:** Biosynthesis of zinc sulfide (ZnS) nanoparticles (NPs) using plant extracts is an alternative method to traditional chemical route. In this study, ZnS-NPs was synthesized via two different routes: (i) bio-based method using leaf extract of *Plectranthus barbatus* as a capping agent and (ii) using the chemical co-precipitation route as a capping-free method. The effect of synthesis routes on the structural, morphological, and optical properties of the prepared NPs was analyzed. The obtained ZnS-NPs was characterized using UV-Visible, FTIR, XRD, and SEM. According to XRD analysis, the average crystallite sizes were found to be 2.259 and 3.080 nm for chemically and bio-synthesized ZnS, respectively; while SEM revealed aggregated NPs to be counted. Additionally, the optical energy bandgaps were 3.82 and 3.73 eV of the samples synthesized via chemical and green methods, respectively. The obtained results indicate that ZnS-NPs prepared via the capping-free chemical route is more favored, in term of its morphological and optical properties, compared to the sample prepared by green method.

## CONTENTS

1. Introduction
2. Materials and Methods
3. Results and Discussion
4. Conclusions
5. References

## 1. Introduction

Nanomaterials play a very important role in today's material world. They show individual and different biological, chemical and physical

properties when compared to their bulk counterparts [1, 2]. Nanoparticles (NPs) are widely investigated for their electrical, optical, thermal, spectral, and antibacterial properties. Due to their nanosize, inorganic nanoparticles

have gained considerable attention over the last decade, as their structures possess new and enhanced chemical, physical, and biological properties.

Recently, various metal sulfides including CdS, MgS, and ZnS have been prepared.[3-6]. Among these metal sulfides, ZnS NPs are of greatest interest as they are safe, inexpensive, simple and can be easily synthesized. It is a multi-purpose semiconductor material which possesses attractive properties such as large bandgap (3.68 eV), high exciton bonding energy (38 meV), and eco-friendly features [7-9]. As a result, it became a useful in various fields including electronics, communication, solar cell, photocatalytic and biological applications [10-14]. Numerous physical and chemical routes have been utilized to prepare ZnS NPs, such as, sonochemical, sol-gel, co-precipitation, and solvothermal route [9-12]. However, these routes are costly and potentially hazardous to the environment and living organisms. Chemical methods commonly involve chemicals those are toxic for living organism and non-environmentally friendly [12,13]. Commonly, the traditional chemical and physical techniques require additional capping and stabilizing agent for NPs production, those mostly applied as organic solvents and reducing agents [13-18]. Therefore, there is a clear requirement for an alternative cost-effective, and safe and environmentally sound route for NPs synthesis.

Hence, biosynthesis seems to be the alternative solution which featured with many advantages for the environment, and of which is the use of toxic-free materials in the preparation process. Typically, metal oxide NPs can be biosynthesized using plant-extract with certain type of extract source as well as their concentrations may employed for tailoring the NPs sizes, shapes and morphologies, and further direct their applications. Many researchers have been biosynthesized ZnS-NPs using plants extracts, which have protruded as an alternative to the chemical synthetic protocol, providing simple processes with natural covering agents [15, 16]. However, some issues related to biosynthesis route were also reported, like the stability and aggregation,

control of crystal growth, distribution and morphologies, which are important and necessitate true solution.

In this work, we prepared ZnS-NPs using the chemical and green route, then their structural, morphological, and optical properties were compared. SEM, XRD, FTIR and UV-Visible techniques were used for material characterization. The produced NPs via both techniques have shown different size, bandgap and morphology.

## 2. Materials and Methods

### 2.1 Materials

*Plectranthus barbatus* leaves (PBL), Zinc nitrate hexahydrate ( $\text{Zn}(\text{NO}_3)_2 \cdot 6\text{H}_2\text{O}$ ;  $\geq 98.5\%$ ), sodium sulfide ( $\text{Na}_2\text{S}$ ; 97%), and ethanol were procured from BDH Chemical Ltd. All chemicals were used as received unless stated otherwise and distilled water ( $\text{dH}_2\text{O}$ ) was utilized wherever needed.

### 2.2 Methods

#### (i) Green Synthesis

Fresh PBL were collected, during summer season 2021, from Anis district, Dhamar governorate, Yemen. They were washed several times, severely, with tap water and distilled water, cut into small pieces, placed in a mortar and finally ground to obtain dough mass. To prepare extract, a weight of 16 g of this PBL dough was immersed in 250 mL  $\text{dH}_2\text{O}$  and stirred for 90min at room temperature (RT). While mixing, the mixture changed from colorless to brown which then filtered and immediately used for preparation of intended NPs. 25 mL of aqueous leaves extract (PBE) was taken and pour into 100 mL beaker. The flask was put on a magnetic stirrer; then, 8.18 g of zinc nitrate was added at room temperature (RT;  $22 \pm 2$  °C) with constant stirring. Also, 2.14 g of  $\text{Na}_2\text{S}$  was mixed in 25 mL of PBE at RT in 100 mL flask. The two solutions were then mixed with constant stirring at RT for 60 min, during which the color was changed to brown and precipitate. The precipitate was filtered, washed

twice with dH<sub>2</sub>O and ethanol and dried at RT for 48 hrs. After that, the powder was collected into a crucible and dried in 100 °C oven for 90 min. The obtained brown powder was ground using mortar and pestle, and finally the fine powder was stocked for further characterizations.

### (ii) Chemical method

ZnS-NPs was fabricated using a chemical co-precipitation route, at RT. All starting chemicals, involving zinc nitrate and sodium sulfide were utilized without any further purification. 8.18 g of zinc nitrate hexahydrate was dissolved in 25 mL dH<sub>2</sub>O and stirred for 15 mint to achieve clear solution. 2.14 g of Na<sub>2</sub>S was also dissolved in 25 mL of dH<sub>2</sub>O and stirred for 15 min. After that, aqueous solutions of Na<sub>2</sub>S was injected into the above zinc nitrate solution till the color changed to white. The mixture was stirred for 60 min at RT by using a magnetic stirrer in order to obtain a homogenous mixture. The precipitate was

filtered and washed twice with dH<sub>2</sub>O and ethanol in order to eliminate impurities. The precipitates were dried in oven at 100 °C for 90 min. Finally, fine powder was stocked for further characterizations.

### 2.3 Characterization

FTIR spectra were obtained in a Nicolet iS10 spectrometer (WI, USA) on the range of 600–4000 cm<sup>-1</sup>. The XRD profiles were collected via XD-2 X-ray diffractometer (China) with CuK $\alpha$ 1 radiation of wavelength ( $\lambda$ ) = 1.54 Å in the two-theta ( $2\theta$ ) degree of 15–80 and at 0.02 min<sup>-1</sup>. The UV-Vis analysis was carried out using a Hitachi U-3900 (Japan) on the range of 200–900 nm at RT. The surface morphology imaging was performed on SEM (JSM-6360 LV-Japan).

## 3. Results and Discussion

### 3.1 XRD analysis

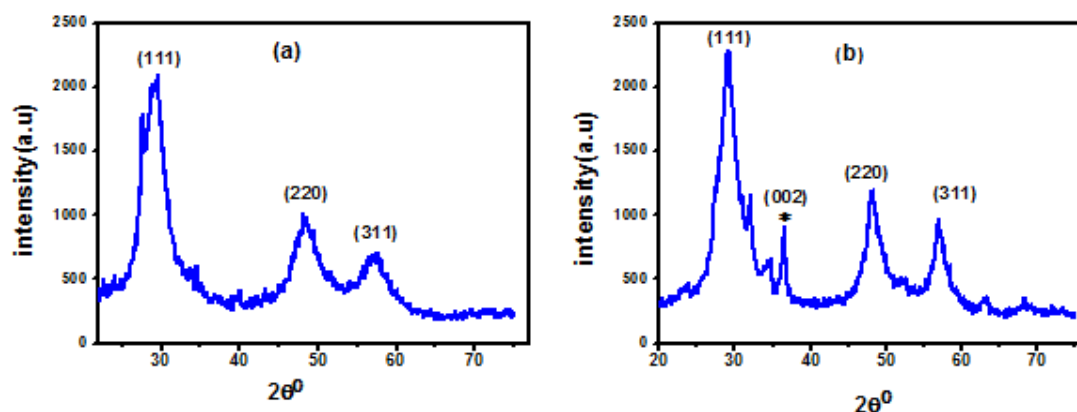


Fig.1 (a) XRD of nano ZnS by chemical route, (b) XRD of nano ZnS by green route.

The purity and crystal phase of ZnS-NPs were characterized via XRD. Fig.1a displays the XRD pattern of ZnS-NPs prepared via chemical route. From the Fig.1, it could be deduced that the prepared ZnS-NPs are in pure phase. The peaks obtained at two-theta ( $2\theta$ ) values of 27.54, 47.23 and 55.79 can be attributed to the planes (111), (220) and (311) respectively. All peaks agree with cubic phase of ZnS that matched with

(JCPDS 05-0566). Broadening in the X-ray diffraction peaks could be seen very clearly, that emphasizes the NPs nature of ZnS-NPs. Fig.1b displays XRD pattern of ZnS-NPs using bio-synthesis route. Broad diffraction peaks were seen for eco-friendly route with new diffraction peak was indexed at  $2\theta$  value of 36.51 to the planes (002). This characteristic diffraction peak correspond to hexagonal ZnS (JCPDS Card No. 04-0831). In addition, some extra peaks at  $2\theta$  values 32.10 and 34.92 may indicate organic

compounds present in the aqueous extract [17]. The broadening exists in all the peaks is due to the smaller crystallite size. The intensity in the signal of their diffraction patterns is decreased because of broadening of peaks. For the two samples the average grain size (D) was calculated from the X-ray diffraction pattern parameters via Scherrer's relation  $D = 0.9\lambda/\beta\cos\theta$ , [18, 19]. The broadening in peaks because of crystal imperfection, distortion and micro-strain was computed by the relation  $\varepsilon = \beta \cos\theta/4$  [4]. Also,

the average dislocation density was calculated using the equation  $\delta = \frac{1}{D^2}$ [20]. Stacking fault (SF) was calculated via the relation  $SF = [\frac{2\pi^2}{45(3\tan\theta)^{0.5}}]\beta$ [4]. The calculated results are shown in the corresponding table.

Table 1. XRD parameters of ZnS obtained using chemical and biosynthesis routes

Method	2-theta ( $2\theta^\circ$ )	(hkl)	FWHM ( $\beta$ )	d-spacing ( $\text{\AA}$ )	crystallite size D(nm)	Average(D; nm)	Average dislocation density (lines/m <sup>2</sup> )*10 <sup>17</sup>	Micro-strain( $\varepsilon$ )	SF
Chemical method	29.09	(111)	3.764	3.07	2.181	2.259	1.959	0.0158	0.0326
	48.59	(220)	4.043	1.87	2.156			0.0161	0.0265
	56.98	(311)	3.705	1.61	2.439			0.0142	0.0222
Green method	29.27	(111)	3.549	3.05	2.313	3.080	1.054	0.0149	0.0306
	48.41	(220)	2.927	1.88	2.975			0.0116	0.0193
	57.72	(311)	2.296	1.59	3.951			0.0088	0.0137

The table illustrates the crystallite size, d-spacing, stacking fault (SF), density of dislocation and micro-strain of ZnS-NPs prepared from green and chemical routes. As can be seen, the average D values for the chemically and bio-synthesized ZnS were 2.259 and 3.080 nm, respectively.

### 3.2 SEM analysis

The surface morphology of the prepared ZnS-NPs was analyzed using SEM. Fig. 2(a and b) displays

the SEM micrographs of ZnS obtained from the applied chemical and green routes, respectively. As can be seen, ZnS NPs fabricated via the chemical route revealed NPs with ranges of sizes and shapes, mostly of spherical type. Furthermore, it is observed that many of the particles are agglomerated. On the other hand, ZnS NPs synthesized by green method are highly agglomerated compared to the ones obtained from chemical method, with a curly hair-like structure. The variation in the surface morphology indicate the effect of synthesis route in the end-properties of the produced NPs, which further govern their applications.

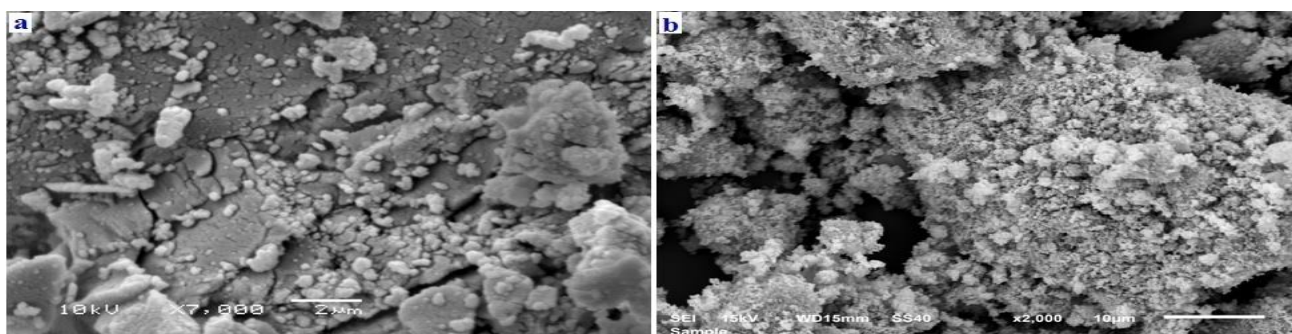


Fig 2. (a) SEM image of ZnS-NPs using chemical route. (b) SEM image of ZnS-NPs using green route.

### 3.3 UV-Visible analysis

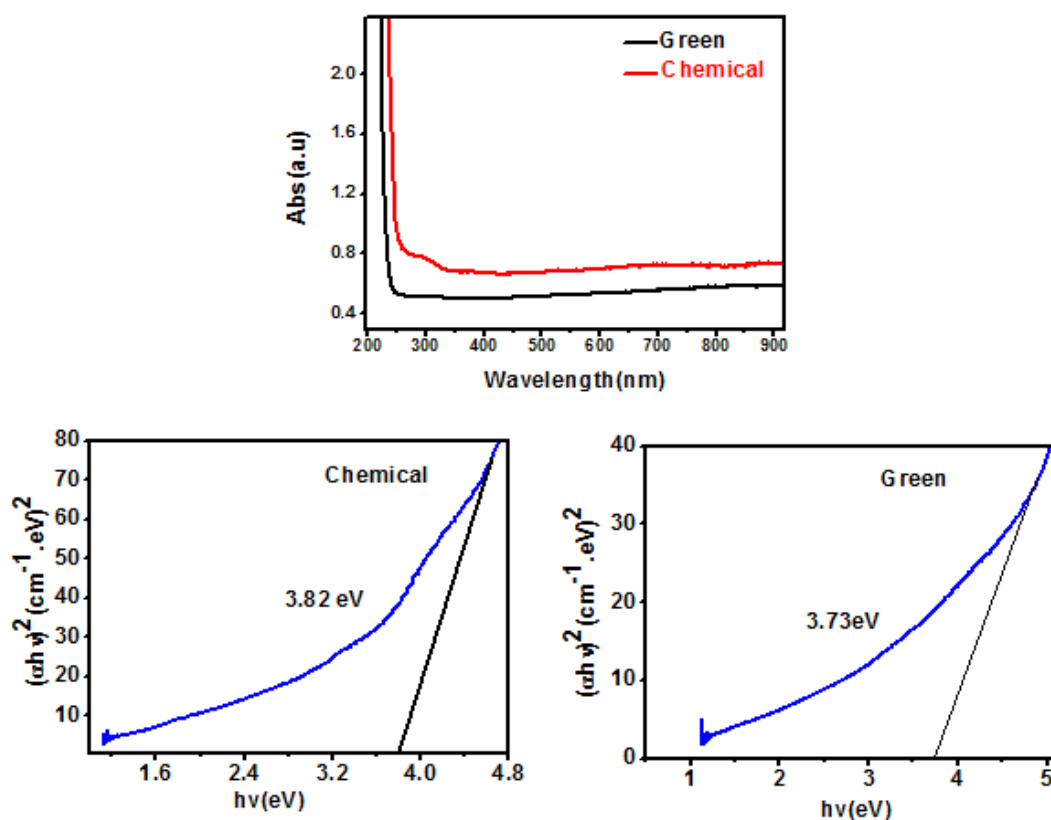


Fig. 3 Absorption spectra and optical energy gap of samples prepared via chemical and green route.

The UV–Vis spectra of ZnS-NPs prepared via chemical and bio-synthesis routes as a function of  $\lambda$  are given in Fig.3, and presented on the range 200–900 nm. It shows that the optical absorption decrease as wavelength increases. In both cases, the absorption band displays a blue shift because of the quantum confinement effect, as compared with the bulk [28]. The coefficient of absorption ( $\alpha$ ) associated with the strong absorption region for the two samples of ZnS-NPs were computed from sample thickness ( $d$ ) and absorbance ( $A$ ) using the equation  $\alpha = 2.303A/d$  [21]. The Tauc's formula  $(\alpha h\nu) = (h\nu - E_g)^n$ , was utilized to calculate the optical bandgap ( $E_g$ ) of ZnS-NPs [22]. The obtained energy bandgap was 3.82 eV for chemically synthesized ZnS-NPs and 3.72 eV for the one from the green route. In the two cases, the energy bandgap was higher than the standard

value of 3.68 eV. The bandgap increase of ZnS-NPs with reduction in the crystallite size might be a result of quantum confinement effect.

### 3.4 FTIR analysis

Figure.4 displays the FTIR spectra for ZnS-NPs synthesized via chemical and green methods. The samples display close spectra with few differences. The peaks at 688, and 936 are assigned to the Zn-S band in both the cases [23]. The Peak observed at 1023  $\text{cm}^{-1}$  may indicate C-O bonds [3]. The absorption band at 1319  $\text{cm}^{-1}$  and 1386  $\text{cm}^{-1}$  coincides to C-C bond [4, 24]. The Peaks observed on the range of 1971–2600  $\text{cm}^{-1}$  are instrument-based background [4, 24]. The broad peak at 3407  $\text{cm}^{-1}$  is due to hydroxyl group stretching and the band at 1641  $\text{cm}^{-1}$  is

due to hydroxyl group bending of adsorbed moisture in the sample (green method) and each the other peaks are attributed to the characteristic of the material [17, 25]. The peak in the region between  $1548\text{ cm}^{-1}$  coincides to alkene groups [26].

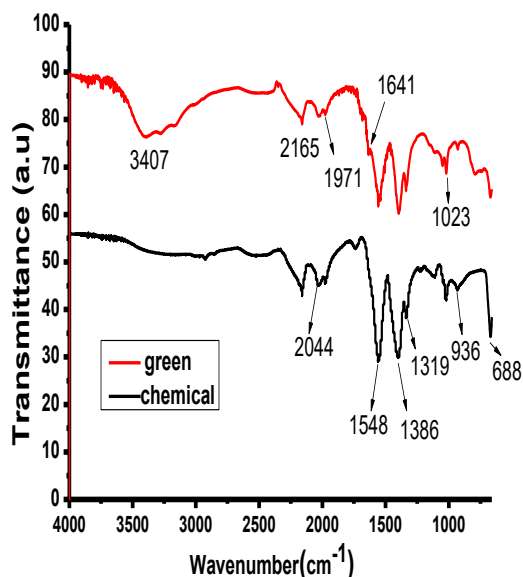


Fig.4 FTIR spectra of ZnS-NPs obtained via chemical and green methods

#### 4. Conclusions

ZnS-NPs have been successfully prepared using two methods, namely green route via zinc nitrate and leaf extract of *Plectranthus barbatus* and co-precipitation route with no capping agent used. XRD revealed the growth of the ZnS-NPs in cubic structure. The average size ( $D$ ) was found as 2.25 and 3.08 nm for ZnS NPs synthesized by co-precipitation and green methods, respectively. SEM image revealed spherical NPs agglomerated into higher sizes and being more visible for biogenic-based NPs. Blue-shift in the FTIR bands was observed in both spectra. The bandgaps for chemically synthesized ZnS was 3.82 eV compared to the biosynthesized one of 3.73 eV. These results proven better or favored properties for chemically synthesized ZnS NPs compared to the biosynthesized one, supporting its potential future application for NPs production.

#### Reference

- [1] S. Velusubhash, K. Kalirajan, S. Harikengaram, R. Vettumperumal, R. Murugesan, Influence of Co-Dopant on Structural, Optical and Electrochemical Properties of Zinc Sulphide Quantum Dots Journal of Nanoscience and Technology 4(2018) 461-466. <https://doi.org/10.30799/jnst.143.18040501>.
- [2] M.M. El-Desoky, G.A. El-Barbary, D.E.E. Refaey, F. El-Tantawy, Optical constants and dispersion parameters of La-doped ZnS nanocrystalline films prepared by sol-gel technique, Optik - International Journal for Light and Electron Optics, 168 (2018) 764-777. <https://doi.org/10.1016/j.ijleo.2018.04.129>.
- [3] T.P. Nguyen, Q.V. Lam, T.B. Vu, Energy transfer in poly(vinyl alcohol)-encapsulated Mn-doped ZnS quantum dots, Journal of Luminescence, 203 (2018) 533-539. <https://doi.org/10.1016/j.lumin.2018.07.010>.
- [4] M. Jothibas, C. Manoharan, S.J. Jeyakumar, P. Praveen, I.K. Punithavathy, J.P. Richard, Z. A, Synthesis and enhanced photocatalytic property of Ni doped ZnS nanoparticles, Solar Energy 159 (2018) 434-443. <https://doi.org/10.1016/J.solener.2017.10.055>
- [5] M.M. Ba-Abbad, M.S. Takriff, Abdelbaki Benamor, Ebrahim Mahmoudi, Abdul Wahab Mohammad, Arabic gum as green agent for ZnO nanoparticles synthesis: properties, mechanism and antibacterial activity, Materials Science: Materials in Electronics 28 (2017) 12100-12107. <https://doi.org/10.1007/s10854-017-7023-2>
- [6] R. Rajeswari, T. Pitchai, R. Thangamuthu, S. Sridhar, V. Alagan, Green synthesis of ZnO nanoparticles using Carica papaya leaf extracts for photocatalytic and photovoltaic applications Materials Science: Materials in Electronics 28 (2017) 10374-10381. <https://doi.org/10.1007/s10854-017-6807-8>
- [7] B. Poornaprakash, P.T. Poojitha, U. Chalapathi, K. Subramanyam, S.-H. Park, Synthesis, structural, optical, and magnetic properties of Co doped, Sm doped and Co,Sm co-doped ZnS nanoparticles, Physica E, (2016) 180-185. <https://doi.org/10.1016/J.physe.2016.05.025>
- [8] A. Al-Sharabi, A. Alnehia, A. AL-Osta, N.A.A. Yahya, Effect of Copper Doping on Structural and Optical Properties of Zinc Sulfide (ZnS) Nanoparticles, Al-Baydha University Journal for Researches 1(2019) 224-234. <https://doi.org/10.5680/buj.v1i2.25>
- [9] J. Sharma, A. Gupta, O.P. Pandey, Effect of Zr doping and aging on optical and photocatalytic properties of ZnS nanopowder Ceramics International, 45 (2019) 13671-13678. <https://doi.org/10.1016/J.ceramint.2019.04.061>

- [10] H.R. Rajabi, M. Farsi, Effect of transition metal ion doping on the photocatalytic activity of ZnS quantum dots: Synthesis, characterization, and application for dye decolorization, *Journal of Molecular Catalysis A: Chemical*, 399 (2015) 53-61. <https://doi.org/10.1016/J.molcata.2015.01.029>
- [11] S. Kumar, H.C. Jeon, T.W. Kang, R. Singh, J.K. Sharma, R.K. Choubey, Structural and optical properties of silica capped ZnS:Mn quantum dots, *J Mater Sci: Mater Electron* 26 (2015) 3939–3946. <https://doi.org/10.1007/s10854-015-2928-0>
- [12] S. Horoz, Q. Dai, F.S. Maloney, B. Yakami, J.M. Pikal, X. Zhang, J. Wang, W. Wang, J. Tang, Absorption Induced by Mn Doping of ZnS for Improved Sensitized Quantum-Dot Solar Cells, *PHYSICAL REVIEW APPLIED* 3(2015). <https://doi.org/10.1103/physRevApplied.3.024011>
- [13] B. Poornaprakash, S. Ramu, S.-H. Park, R.P. Vijayalakshmi, B.K. Reddy, Room temperature ferromagnetism in Nd doped ZnS diluted magnetic semiconductor nanoparticles, *Materials Letters* 164 (2016) 104–107. <https://doi.org/10.1016/J.matlet.2015.10.119>
- [14] H.Q. Alijani, S. Pourseyedi, M. Torkzadeh-Mahani, M. Khatami, Green Synthesis of Zinc sulfide (ZnS) Nanoparticles using Stevia rebaudiana Bertoni and evaluation of its cytotoxic properties, *Journal of Molecular Structure*, 1175 (2019). <https://doi.org/10.1016/J.molstruc.2018.07.103>
- [15] A. Al-Sharabi, A. Alneha, A.H. Al-Hammadi, K.A. Alhumaidha, A. AL-Osta, The effect of Nigella sativa seed extract concentration on crystal structure, band gap and antibacterial activity of ZnS-NPs prepared by green route, *J Mater Sci: Mater Electron*, 33 (2022) 20812-20822. <https://doi.org/10.1007/s10854-022-08890-7>
- [16] U.S. Senapati, R. Athparia, Green synthesis of ZnS nanoparticles using allium sativum l. extract and study of their structural, optical and electrical properties, *Chalcogenide Letters*, 19 (2022) 203-216. <https://doi.org/10.15251/CL.2022.193.203>
- [17] Senapati, U.S., Jha, D.K. and Sarkar, D. Green Synthesis and Characterization of ZnS nanoparticles *Research Journal of Physical Sciences*, 1 (2013) 1-6. [Dio:10.4236/ajps.2018.96094](https://doi.org/10.4236/ajps.2018.96094)
- [18] M.M. Khan, M.H. Harunsani, A.L. Tan, M. Hojamberdiev, S. Azamay, N. Ahmad, Antibacterial activities of zinc oxide and Mn-doped zinc oxide synthesized using Melastoma malabathricum (L.) leaf extract *Bioprocess and Biosystems Engineering* 43 (2020) 1499-1508. <https://doi.org/10.1007/s00449-020-02343-3>.
- [19] M.M. Khan, M.H. Harunsani, A.L. Tan, M. Hojamberdiev, Y.A. Poi, N. Ahmad, *Antibacterial Studies of ZnO and Cu-Doped ZnO Nanoparticles Synthesized Using Aqueous Leaf Extract of Stachytarpheta jamaicensis*, *BioNanoScience*, 10 (2020) 1037–1048. <https://doi.org/10.1007/s12668-020-00775-5>
- [20] A.B. Alwany, G.M. Youssef, E.E. Saleh, O.M. Samir, M.A. Algradee, A. Alneha, Structural, optical and radiation shielding properties of ZnS nanoparticles QDs *Optik - International Journal for Light and Electron Optics*, 260 (2022) 169124. <https://doi.org/10.1016/J.ijleo.2022.169124>
- [21] A. Al-Sharabi, K.S.S. Sada'a, A. AL-Osta, R. Abd-Shukor, Structure, optical properties and antimicrobial activities of MgO–Bi<sub>2-x</sub>Cr<sub>x</sub>O nanocomposites prepared via solvent-deicient method, *Scientific Reports*, 12 (2022) 10647. <https://doi.org/10.1038/s41598-022-14811-9>.
- [22] A. AL-Osta, A. Alneha, A.A. Qaid, H.T. Al-Ahsab, A. Al-Sharabi, Structural, morphological and optical properties of Cr doped ZnS nanoparticles prepared without any capping agent, *Optik - International Journal for Light and Electron Optics*, 214 (2020) 164831. <https://doi.org/10.1016/J.ijleo.2020.164831>.
- [23] S.C. Tudu, M. Zubko, J. Kusz, A. Bhattacharjee, Structural, morphological and optical characterization of green synthesized ZnS nanoparticles using Azadirachta Indica (Neem) leaf extract, *International Journal of Nano Dimension*, 11 (2020) 99-111. [corpus ID:216547618](https://doi.org/10.1007/s10854-020-02343-3)
- [24] N.A. Al-Shabib, F.M. Husain, F. Ahmed, R.A. Khan, I. Ahmad, E. Alsharaeh, M.S. Khan, A. Hussain, M.T. Rehman, M. Yusuf, I. Hassan, J.M. Khan, G.M. Ashraf, A.M. Alsalmeh, M.F. Al-Ajmi, V.V. Tarasov, G. Aliev, Biogenic synthesis of Zinc oxide nanostructures from Nigella sativa seed: Prospective role as food packaging material inhibiting broad-spectrum quorum sensing and biofilm, *Scientific RepoRts* 6(2016) 36761. <https://doi.org/10.1038/srep36761>
- [25] M. Sathishkumar, M. Saroja, M. Venkatachalam, Influence of (Cu, Al) doping concentration on the Structural, Optical and Antimicrobial Activity of ZnS Thin Films Prepared by Sol-Gel dip coating Techniques, *Optik - International Journal for Light and Electron Optics*, 182 (2019) 774-785. <https://doi.org/10.1016/J.ijleo.2019.02.014>
- [26] V. Kamath, P. Chandra, G.P. Jeppu, Comparative study of using five different leaf extracts in the green synthesis of iron oxide nanoparticles for removal of arsenic from water, *International Journal of Phytoremediation*, 22 (2020) 1278-1294. [doi:10.1080/15226514.2020.1765139](https://doi.org/10.1080/15226514.2020.1765139).